RSC Advances

This is an *Accepted Manuscript*, which has been through the Royal Society of Chemistry peer review process and has been accepted for publication.

Accepted Manuscripts are published online shortly after acceptance, before technical editing, formatting and proof reading. Using this free service, authors can make their results available to the community, in citable form, before we publish the edited article. This *Accepted Manuscript* will be replaced by the edited, formatted and paginated article as soon as this is available.

You can find more information about *Accepted Manuscripts* in the **Information for Authors**.

ROYAL SOCIETY
OF **CHEMISTRY**

www.rsc.org/advances

Synthesis, Micellization, and Thermally-Induced Macroscopic Micelle Aggregation of Poly(vinyl chloride)-*g*-poly(*N*-isopropylacrylamide) Amphiphilic Copolymer

Keyong Liu, Pengju Pan,* Yongzhong Bao*

State Key Laboratory of Chemical Engineering, College of Chemical and Biological Engineering, Zhejiang University, 38 Zheda Road, Hangzhou 310027, China

*Corresponding author

E-mail*: yongzhongbao@zju.edu.cn (Y. Bao); panpengju@zju.edu.cn (P. Pan)

1

Abstract: A series of poly(vinyl chloride)-*g*-poly(*N*-isopropylacrylamide) (PVC-*g*-PNIPAM) amphiphilic copolymers with different graft lengths and densities were synthesized via the single electron transfer-living radical polymerization (SET-LRP) of NIPAM using the poly(vinyl chloride-*co*-allyl α-bromoisobutyrate) as macroinitiator. The living nature of SET-LRP grafting copolymerization was verified by the kinetics study and narrow molecular weight distribution of PNIPAM grafts. Chemical structure, micellation, and thermally-induced multistep aggregation of PVC-*g*-PNIPAMs were investigated. PVC-*g*-PNIPAMs form micelles comprised of the PVC core and PNIPAM corona in water at room temperature. These micelles are thermoresponsive and show the lower critical solution temperature (LCST). Micelle size and LCST of PVC-*g*-PNIPAM increase with increasing the graft density and length of PNIPAM. PVC-*g*-PNIPAM exhibits a very unique aggregation behavior above LCST and it forms a three-dimensional macroscopic aggregate with the well-defined and tunable shape at an extremely low concentration (~0.1 wt%). The aggregate shrinks to a more compact structure with the further increase of temperature. Higher copolymer concentration, longer graft length, and lower graft density are favorable for the macroscopic micelle aggregation of PVC-*g*-PNIPAMs. A self-standing and superporous PVC-*g*-PNIPAM material having an extremely low density of ~ 0.01 g/cm^3 and a high porosity of > 99% is attained after freeze-drying the micelle aggregate.

Keywords: poly(vinyl chloride); poly(*N*-isopropylacrylamide); graft copolymer; micelle; aggregation

Introduction

Amphiphilic copolymers, having a great solubility difference between the hydrophilic and hydrophobic segments, can self-assemble into the micelles and

micelle aggregates with nanometer or submicrometer scales in an aqueous media. They have attracted increasing academic interests because of their wide range of potential applications in the drug delivery, tissue engineering, membrane science, and nanotechnology.[1–4] Recently, the stimuli-responsive amphiphilic copolymers and their self-assemblies have been received much attentions because of their unique properties. Poly(*N*-isopropylacrylamide) (PNIPAM) is one of the most studied thermoresponsive polymers and exhibits a reversible thermoresponsive phase transition in aqueous solution around the lower critical solution temperature (LCST).[5,6] PNIPAM is water-soluble, hydrophilic and exists in an extended chain conformation below LCST, while it changes to insoluble and hydrophobic as the temperature exceeds LCST.

Incorporating the hydrophobic segment in PNIPAM can change its LCST and phase transition behavior and also prepare the thermoresponsive copolymer micelles. With the development of controlled/living free radical polymerization (CLRP), many well-defined amphiphilic diblock,[7–13] triblock,[14–21] star-shaped block,[22–26] and graft[27–32] copolymers consisting of the PNIPAM segments have been prepared and their self-assembling, thermoresponsive behavior have been investigated. These linear and star-shaped block copolymers can be synthesized with combination of the CLRP of *N*-isopropylacrylamide (NIPAM) and the living polymerization of other monomers, in which the chain end functionalization of the first block is necessary for initiating the polymerization of second block. To synthesize the amphiphilic graft copolymers containing PNIPAM grafts, the functionalization of polymer backbone is required. Then, PNIPAM can be grafted onto the backbone via the CLRP of NIPAM using the functionalized polymer backbone as macroinitiator[27–29] or the click reaction between functionalized PNIPAM and polymer backbone,[31,32] which correspond to the "grafting-from" and "grafting-to" strategies, respectively. For example, Wu *et al*. have

3

synthesized the well-defined graft copolymers with PNIPAM side chains on the random acrylate copolymer backbone with a combination of the atom transfer radical polymerization (ATRP), click chemistry, and reversible addition-fragmentation chain transfer (RAFT) polymerization.[28] Jiang *et al.* have prepared the poly(glycidyl methacrylate)-*g*-PNIPAM copolymers with different graft lengths and densities by CLRP and click chemistry.[30] Li et al. have synthesized the poly(ε-caprolactone)-*g*-PNIPAM (PCL-*g*-PNIPAM) copolymers with the combination of ring-opening polymerization, ATRP, and click chemistry using the grafting-from and grafting-to strategies.[31,32]

The amphiphilic copolymers containing hydrophilic PNIPAM segments can form the core-shell micelles or vesicles in aqueous solution below LCST. These self-assembled nanoparticles are thermoresponsive and undergo aggregation as the temperature is increased to above LCST, due to the hydrophilic-to-hydrophobic transition of PNIPAM segments.[13,15,19,22,31,32] These micelle solution usually change from transparent to turbid upon heating to above LCST, due to the formation of micelle aggregate or precipitate with larger size. The aggregation of micelles would be a feasible way to prepare the macroscopic materials (*e.g.*, physical gel, aerogel) with the well-defined nanostructure. However, the macroscopic shapes of micelle aggregates for the thermoresponsive amphiphilic copolymers in dilute solution (*e.g.*, < 1 wt%) are generally uncontrollable and ill-defined, because it is difficult to control the attractions and aggregation degree between micelles in a macroscopic scale.

Poly(vinyl chloride) (PVC) is one of the most widely used polymers in the world due to its good price/performance balance and variable mechanical properties.[33] In order to modify the wettability, hydrophilicity, and biocompatibility of PVC, the grafting of PNIPAM onto PVC have been studied. NIPAM has been grafted onto PVC

backbone using the conventional free-radical copolymerization in solution[34–36] or under irritation.[37] However, these procedures cannot prepare the graft copolymers with the well-controlled structures such as graft length and density. In contrast, CLRP has been an efficient method to prepare the grafting copolymers of PVC with well-defined structures. Graft copolymers with PVC backbones have been prepared by two approaches. One is to graft from the inherent structural defects (*e.g.*, allyl chloride, tertiary chloride groups) in PVC[38] and the other is the preparation of a macroinitiator by copolymerization of vinyl chloride (VC) with a monomer containing an CLRP initiating group (*e.g.*, vinyl chloroacetate).[39] The latter method is considered to be more effective to synthesize the PVC-*g*-PNIPAM amphiphilic graft copolymers with the defined chemical structures, because the content of initiating sites can be controlled. On the other hand, PVC is more hydrophobic and has larger density compared to the polyacrylates and aliphatic polyesters, which have been widely used as the hydrophobic segments to copolymerize with PNIPAM.[7–11,13–19,22,23,31,32] This may induce the unique phase transition and aggregation behavior of PVC-*g*-PNIPAM thermoresponsive micelles compared to the micelles of other thermoresponsive amphiphilic copolymers bearing PNIPAM segments.[13,15,19,22,31,32]

In this work, a series of PVC-*g*-PNIPAM amphiphilic copolymers with controlled length and density of PNIPAM grafts were synthesized by single electron transfer-living radical polymerization (SET-LRP) of NIPAM using the poly(vinyl chloride-*co*-allyl-2-bromoisobutyrate) [P(VC-*co*-ABiB)] random copolymer as macroinitiator. Polymerization kinetics, chemicals structure, micellation, thermoresponsive and micelle aggregation behavior of PVC-*g*-PNIPAMs were investigated. It is found that PVC-*g*-PNIPAM micelles form the macroscopic

5

aggregate with well-defined and controllable three-dimensional (3D) shapes in the dilute solution at a temperature above LCST. The thermally-induced aggregation process and microstructure of PVC-*g*-PNIPAM micelles were also studied.

Experimental part

Materials

VC with a polymerization grade was supplied by Hangzhou Electrochemical Group Co., Ltd., China. NIPAM (Acros) was recrystallized twice from *n*-hexane prior to use. Tris[2-(dimethylamino)-ethyl]amine (Me$_6$TREN) was synthesized according to a published method.[40] Allyl-2-bromoisobutyrate (ABiB, 98%, Aldrich), copper powder (~75 μm powder, 99%, Aldrich), anhydrous copper (II) chloride (99%, Acros), trifluoroacetic acid (TFA, Aladdin), bis-(2-ethylhexyl) peroxydicarbonate (EHP, Arkema), and *tert*-butyl peroxypivalate (Luperox 11, Arkema) were used as received.

Synthesis of P(VC-*co*-ABiB) macroinitiator. ABiB (1.5 g, 7.25 mmol), Luperox 11 (0.12 g), EHP (0.12 g), and 1,4-dioxane (50.0 g) were added into a 200 mL stainless steel tube sealed with the ball valves. The tube was pulped and filled with dry argon for three cycles at 0 °C. 13.5 g (0.216 mol) of VC was then added into the tube. The tube was immersed and rotated in a water bath at 57 °C for 4.5 h for polymerization. After polymerization, the tube was cooled down and slowly opened to remove the unreacted VC. The reaction mixture was poured into methanol (500 mL) and the precipitate was filtered and dried in vacuum to a constant weight. P(VC-*co*-ABiB) macroinitiator was marked as PVC$_x$, in which *x* represents the averaged degree of polymerization (*DP*) of VC.

Synthesis of PVC-*g*-PNIPAM. A typical procedure to synthesize PVC-*g*-PNIPAM copolymer is shown as below. NIPAM (0.9 g, 7.96 mmol), P(VC-*co*-ABiB) (0.5 g, 0.30 mmol of bromide group), CuCl$_2$ (6.2 mg, 0.05 mmol),

Me$_6$TREN (64 mg, 0.28 mmol), and DMF (3.0 g) were added into a 25 mL Schlenk tube. The mixture was degassed by three freeze-pump-thaw cycles, followed by the addition of 0.0178 g (0.28 mmol) of Cu powder. The polymerization was allowed to proceed at 25 °C for 2 h under continuous stirring. After the reaction, the mixture was diluted by 10 mL of THF and precipitated in 100 mL of cold ethyl ether. The precipitate was filtered and dried in vacuum to a constant weight. The synthesized PVC-*g*-PNIPAM copolymers were denoted as PVC$_x$-*g*-PNIPAM$_y$, in which *x* and *y* represent the averaged *DP* of VC in copolymer backbone and the averaged *DP* of PNIPAM in each graft.

To analyze the polymerization kinetics, a portion of sample was withdrawn using an airtight syringe at a certain time interval during the graft polymerization. Conversion of NIPAM in the sample was determined by gas chromatography (GC). To determine the molecular weight of PNIPAM grafts, 70 mg of PVC-*g*-PNIPAM copolymer was dissolved in 2 mL THF containing 0.25 mL TFA and 0.4 mL water. The solution was stirred at 40 °C for 72 h for hydrolysis. After the hydrolytic reaction, the solution was precipitated in cold water and filtered. The filtrate was dried to isolate the PNIPAM grafts.

Preparation of PVC-*g*-PNIPAM Micelles. PVC-*g*-PNIPAM micelles were prepared by a dialysis method. Briefly, 0.1 g of PVC-*g*-PNIPAM copolymer was dissolved in 5 mL of DMF and then dialyzed against deionized water (MWCO = 3500) for 48 h. The water was changed every 6 h. The micelle solution was finally passed through a 0.45 μm pore-sized syringe filter.

Characterization

The concentrations of residual ABiB and NIPAM in the reaction mixture were measured by an Agilent GC (GC-7820A) equipped with a HP-INNOWax capillary

column (30 m × 0.32 mm × 0.25 μm). Toluene was used as an internal standard to calculate the conversions of ABiB and NIPAM. Chemical structure of copolymer was measured on a 500 MHz Bruker DRX500 nuclear magnetic resonance (NMR) at 20 °C using THF-d_8 as the solvent. Fourier transform infrared (FTIR) spectra were measured on a Nicolet 5700 spectrometer with a resolution of 2 cm^{-1}. Molecular weight and molecular weight distribution were determined by a gel permeation chromatography (GPC) equipped with a Waters 1525 HPLC pump, a Waters 2414 refractive index detector, and three Waters UltraStyragel columns covering the molecular weight ranges of 5~600, 30~500, and 10~100 kg/mol, respectively. THF or DMF containing 0.05 M LiBr were used as eluents at a flow rate of 1.0 mL/min. The molecular weights were calibrated using PMMA as the standards. Viscosity-average molecular weight (M_v) of P(VC-co-ABiB) was calculated from the intrinsic viscosity, which was measured by a Ubbelohde viscometer using cyclohexanone as the solvent, according to ASTM D1243-95. Transmittance of copolymer solution was measured on a UV-vis spectroscopy (UV-1800, Shimadzu) equipped with a S-1700 thermoelectric cell holder at the wavelength of 500 nm. Transmittance of PVC-g-PNIPAM copolymer solution (0.3 wt%) was monitored in the heating and cooling processes at a rate of 0.5 °C/min. Hydrodynamic diameter (D_h) of copolymer micelles in water solution (0.3 wt%) was measured at 20 °C by dynamic light scattering (DLS) on a Zetasizer 3000HSA analyzer (Malvern Instruments). Morphology of copolymer micelles was observed on a JEM-1230 transmission electron microscopy (TEM, JEOL) operating at 100 kV. The sample was prepared by depositing the micelle solution (0.3 wt%) on a copper grid, followed by the evaporation of water under ambient conditions. Structure of freeze-dried micelle aggregate was analyzed on a scanning electron microscopy (SEM, Utral55, CorlzeisD,

8

Germany) at an accelerated voltage of 5 kV. The sample was coated by a gold layer before measurement.

Results and discussion

Synthesis of PVC-*g*-PNIPAM copolymers. PVC-*g*-PNIPAM copolymers were synthesized with a combination of conventional free radical polymerization and SET-LRP, as shown in Scheme 1. Even though PVC contains many chlorine groups along the polymer chain, most of these chlorine groups are too inert to initiate the SET-LRP or ATRP. It has been reported that the bromide group is active enough to initiate the SET-LRP of NIPAM.[41–43] Therefore, ABiB units were first incorporated into PVC to prepared the macroinitiator containing the active bromide initiating sites. P(VC-*co*-ABiB) macroinitiator was synthesized via the traditional free radical copolymerization of VC and ABiB in 1,4-dioxane at 57 °C. The bromide contents in P(VC-*co*-ABiB) macroinitiator was tailored by varying the feed ratio of ABiB to VC. Polymerization conditions, copolymer composition, number-averaged molecular weight (M_n), and polydispersity index (PDI) of P(VC-*co*-ABiB) macroinitiator are shown in Table 1. In order to obtain the P(VC-*co*-ABiB) macroinitiator with relative uniform copolymer composition, the total conversion of monomer was controlled to be less than 50%. Conversion of VC was calculated by comparing the weights of used monomer and synthesized polymer. Conversion of ABiB was evaluated through measuring the composition of reaction mixture by GC. The VC/ABiB molar ratio in P(VC-*co*-ABiB) was calculated from the PVC degree of polymerization, conversions of VC and ABiB. As shown in Table 1, M_n and M_v of P(VC-*co*-ABiB) macroinitiator are consistent, both of which decrease with the increase of ABiB content in the feed. As shown in the FTIR spectra (Figure 1a), P(VC-*co*-ABiB) macroinitiator shows an absorption peak at 1734 cm^{-1}, assigned to the stretching vibration of carbonyl group

in ABiB. This result verifies the successful synthesis of P(VC-*co*-ABiB) macroinitiator.
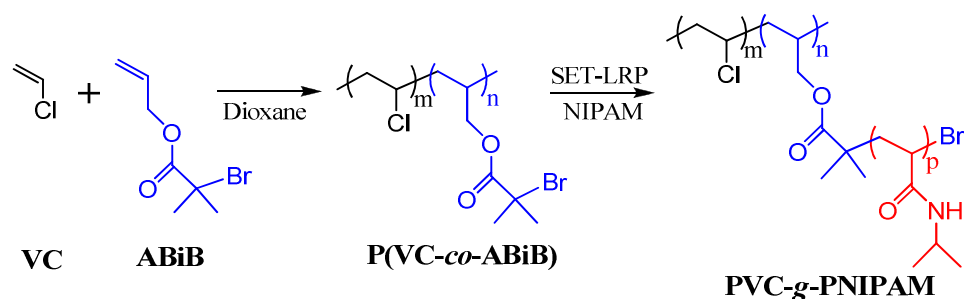
Scheme 1. Synthesis of PVC-*g*-PNIPAM copolymer

Table 1. Polymerization conditions and structural characteristics of P(VC-*co*-ABiB) macroinitiator.

Sample	VC/ABiB molar feed ratio	conv. of VC (%)	conv. of ABiB (%)	VC/ABiB molar ratio in P(VC-*co*-ABiB)	M_n (g/mol)	PDI	M_v (g/mol)
PVC$_{181}$	162/1	39.4	42.6	150/1	11310	1.8	10060
PVC$_{149}$	29.8/1	45.4	26.7	50.7/1	9310	1.7	8190
PVC$_{117}$	13.3/1	30.3	14.0	28.8/1	7310	1.6	6380
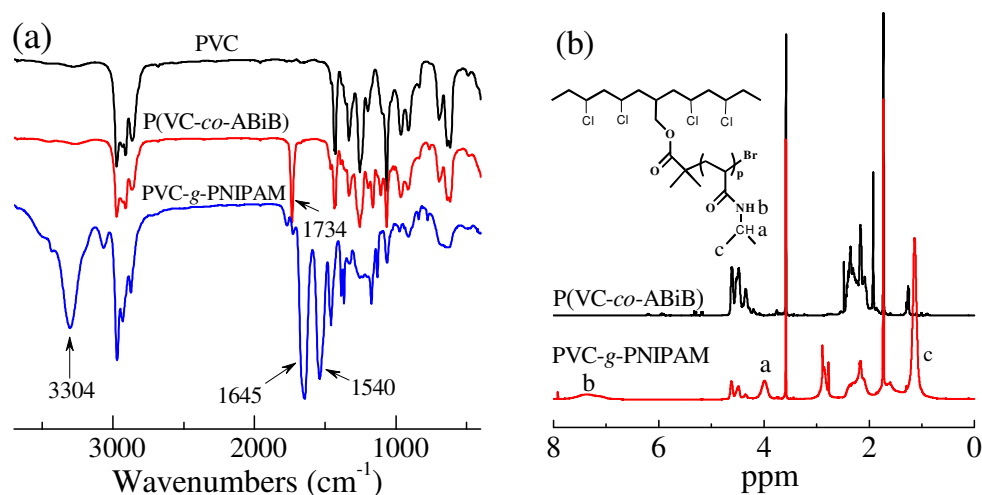
Figure 1. (a) FTIR and (b) ^{1}H-NMR of PVC, P(VC-*co*-ABiB) and PVC-*g*-PNIPAM.

PVC-*g*-PNIPAM graft copolymers were further synthesized by the SET-LRP of NIPAM with P(VC-*co*-ABiB) as the macroinitiator. *In situ* disproportionation of Cu(I)X is an important step in SET-LRP, which regenerates Cu(0) and Cu(II)X$_2$ to

balance and control the polymerization process.[44–46] A small amount of deactivation catalyst $Cu(II)X_2$ is usually used to control the initial step of polymerization. As the polymerization proceeds, the sufficient $Cu(II)X_2$ will be produced by the rapid disproportionation of $Cu(I)X$, allowing for the control over polymerization. Because the content of initiating sites (*i.e.*, bromide groups) in P(VC-*co*-ABiB) backbone was low, excess of $Cu(0)$ was used in the SET-LRP graft polymerization of NIPAM. Polymerization conditions, conversion, and structural characteristics of the synsesized PVC-*g*-PNIPAM copolymers are shown in Table 2.

Table 2. Polymerization conditions and structural characteristics of PVC-*g*-PNIPAMs

PVC-*g*-PNIPAM	[NIPAM]/[Br]/ [Cu(0)]/[Me₆TREN] /[CuCl₂]	Conv. (%)	m_{PNIPAM} (%)	M_n of PNIPAM branches (kg/mol)	PDI of PNIPAM grafts
PVC₁₈₁-*g*-PNIPAM₆₁	275/1/13.8/8.3/1.4	75.2	57.6	15	1.1
PVC₁₈₁-*g*-PNIPAM₉₂	550/1/13.8/8.3/1.4	64.6	69.9	22	1.2
PVC₁₈₁-*g*-PNIPAM₁₀₈	550/1/13.8/8.3/1.4	83.2	75.0	26	1.1
PVC₁₄₉-*g*-PNIPAM₃₆	55/1/2.8/1.7/0.3	70.8	56.1	8.0	1.2
PVC₁₄₉-*g*-PNIPAM₄₆	110/1/1/1.2/0.1	45.6	62.1	14	1.1
PVC₁₄₉-*g*-PNIPAM₈₉	110/1/2.8/3.3/0.6	88.1	76.0	15	1.2
PVC₁₁₇-*g*-PNIPAM₁₇	32/1/1.1/1.1/0.2	59.8	51.9	5.0	1.2
PVC₁₁₇-*g*-PNIPAM₂₇	64/1/0.6/0.7/0.1	46.2	62.4	10	1.2
PVC₁₁₇-*g*-PNIPAM₅₀	64/1/1.6/1.0/0.2	86.3	75.6	13	1.3

In the ^{1}H-NMR spectrum (Figure 1b), PVC-*g*-PNIPAM shows the characteristic resonance peaks at around 1.1, 4.0, and 7.0~8.0 ppm, assigned to the methyl, methine protons of isopropyl groups and amide protons in PNIPAM grafts, respectively. The resonance peaks of PVC backbone decrease in intensity after the graft copolymerization. In the FTIR spectrum (Figure 1a), PVC-*g*-PNIPAM exhibits the characteristic absorptions of PNIPAM at 1645 (C=O stretching), 1540 (N-H bending),[26] and 3304 cm⁻¹ (N-H stretching). The 1734 cm⁻¹ band of ABiB units becomes less obvious in PVC-*g*-PNIPAM, because of the merging with 1645 cm⁻¹

band. As shown in the GPC curves (Figure 2a), PVC-*g*-PNIPAM exhibits single elution peak with a relatively narrow molecular weight distribution. GPC peak shifts to shorter retention time with increasing the NIPAM/Br feed ratio or graft length, indicating the increase of molecular weight.
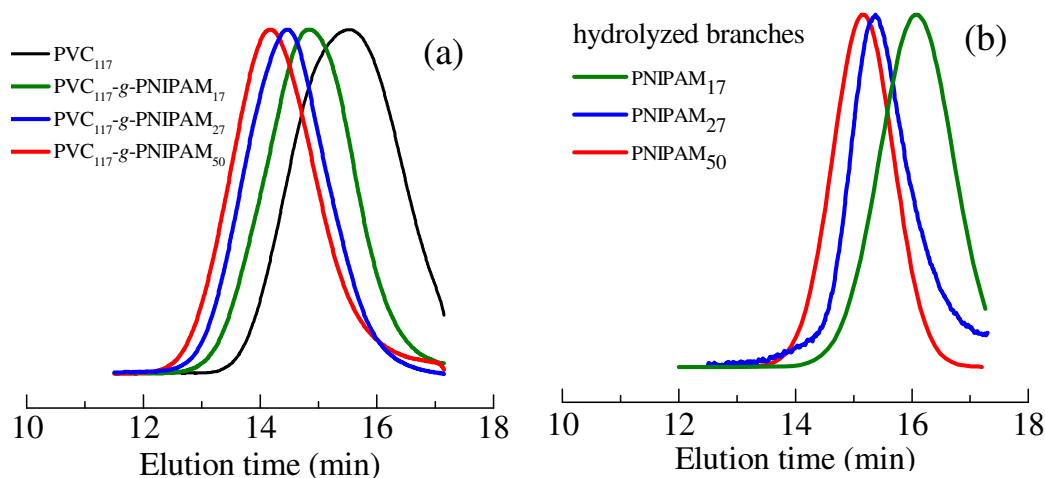
Figure 2. (a) GPC traces of PVC-*g*-PNIPAM and (b) hydrolyzed PNIPAM grafts of PVC-*g*-PNIPAM with the PVC_{117} backbone.

To quantitatively determine the length of PNIPAM grafts, PVC-*g*-PNIPAM was hydrolyzed in the THF/TFA mixed solvent to break the ester bond of ABiB unit and release the PNIPAM grafts. Molecular weights of the hydrolyzed PNIPAM grafts were analyzed by GPC. As shown in Figure 2b, the GPC elution peak shifts toward to the smaller retention time side as the feed ratio of NIPAM to bromide group is increased in graft copolymerization, indicating the increase of graft length. As shown in Table 2, M_ns of graft PNIPAM range from 5.0 to 26 kg/mol and have the PDI values less than 1.3. The mass fraction of PNIPAM grafts (m_{PNIPAM}) in the synthesized PVC-*g*-PNIPAM copolymers are ranging from 50% to 76%, which increases with increasing the feed ratio of NIPAM to bromide group in P(VC-*co*-ABiB) macroinitiator. All the NMR, FTIR, and GPC results confirm the successful synthesis of PVC-*g*-PNIPAM with controllable graft density, length and copolymer

composition.

To confirm the "living" nature of SET-LRP grafting copolymerization, the polymerization kinetics were investigated. Figure 3 shows the changes of NIPAM conversion and $\ln[M]_0/[M]$ with the polymerization time, in which $[M]_0$ and $[M]$ are the concentrations of NIPAM at a time of *0* and *t,* respectively. It can be seen that $\ln[M]_0/[M]$ increases linearly with the polymerization time, in agreement with the typical kinetics of living radical polymerization. Furthermore, the small PDI of PNIPAM grafts can also indicate the "living" characteristics of the SET-LRP grafting copolymerization of NIPAM.
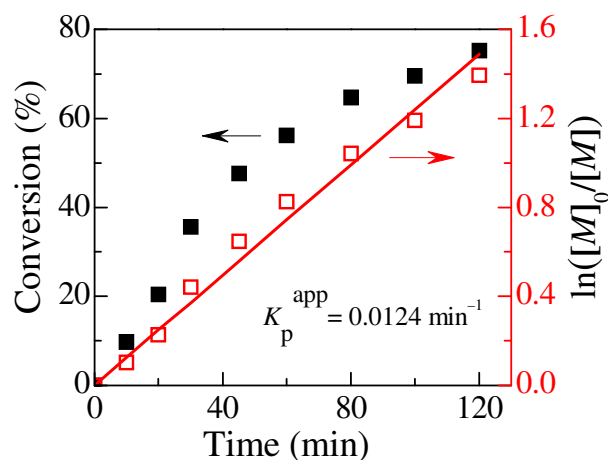
Figure 3. Kinetics plots of SET-LRP of PVC$_{181}$-*g*-PNIPAM$_{108}$

Micellization of PVC-*g*-PNIPAM copolymers. Because the PVC-*g*-PNIPAM copolymers are amphiphilic at room temperature, it is expected that they can self-assemble into the micelles comprised of hydrophobic PVC core and hydrophilic PNIPAM shell in aqueous solution at a temperature below LCST. Since the synthesized PVC-*g*-PNIPAM copolymers are insoluble in water, the copolymer micelles were prepared by a solvent exchange method. PVC-*g*-PNIPAM was first dissolved in DMF and the solvent was gradually changed to water by dialysis. The size and morphology of PVC-*g*-PNIPAM micelles were analyzed by DLS and TEM,

as shown in Figure 4. D_hs of copolymer micelles are ranging in 31~50 nm, which are

dependent on the copolymer composition, graft density and length. As shown in

Figures 4a, at a similar graft length or M_n of PNIPAM graft, the micelle size increases

with the increase of graft density. As shown in Figure 4b, for the graft copolymers

with the same graft density or PVC backbone, the micelle size slightly increases with

increasing the graft length or M_n of PNIPAM graft. This is attributable to the

increased thickness of PNIPAM shell. As shown in the TEM images (Figure 4c), most

of the micelles are spherical and their size is consistent with that determined from

DLS. It is notable that the micelle size shows wide distribution and the large

aggregates with the size more than 100 nm are also observed in TEM analysis. This

may be ascribed to the aggregation of micelles in the preparation of TEM samples.
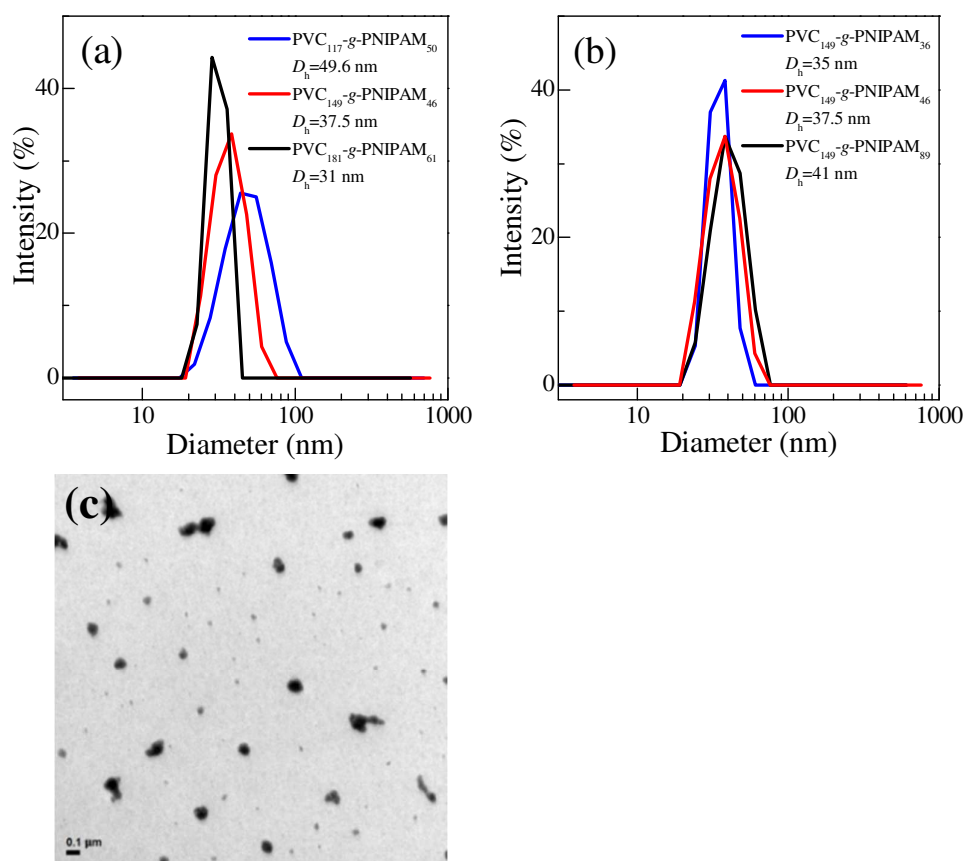
Figure 4. (a, b) Micelle size distribution of PVC-*g*-PNIPAMs with different (a) graft densities and (b) lengths in water at a concentration of 0.3 wt%. (c) Representative

TEM image of PVC_{181}-g-$PNIPAM_{61}$ micelles.

Thermally-induced multistep aggregation of PVC-*g*-PNIPAM micelles.
Because the PNIPAM grafts in micelle shells have LCST behavior, PVC-*g*-PNIPAM micelles would undergo phase transition with the change of temperature. LCST behavior of copolymer micelles was verified from the change of transmittance in the heating process, as shown in Figure 5. As shown in this figure, the micelle solutions of PVC-*g*-PNIPAMs are transparent at a low temperature while it becomes turbid as the temperature increases. The decreased transmittance is ascribed to the aggregation of destabilized micelles. LCSTs of PVC-*g*-PNIPAM micelles are ranging in 28~31 °C, which is lower than that of PNIPAM homopolymer (typically ~ 35 °C).[26] The decreased LCST compared to PNIPAM homopolymer is due to the presence of hydrophobic PVC segment.
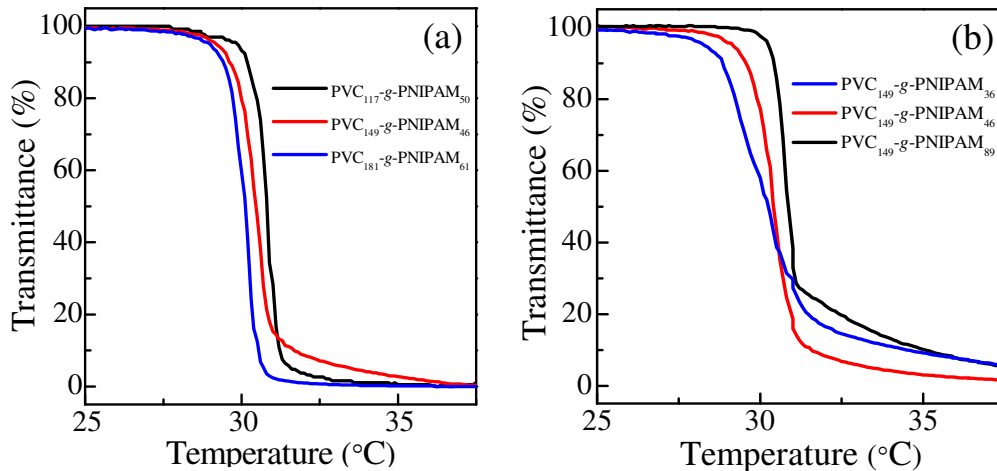
Figure 5. Transmittance-temperature curves for micelle solution (0.3 wt%) of PVC-*g*-PNIPAMs with different (a) graft densities and (b) lengths.

LCST of PVC-*g*-PNIPAM micelles is influenced by the graft density and length. As shown in Figure 5a, LCST increases as the graft density increases when the graft lengths of PVC-*g*-PNIPAMs are similar. Moreover, for the graft copolymers with the

same graft density or PVC backbone, their LCSTs increase with the increase of graft length (Figure 5b). These results are in good accordance with the thermoresponsive graft copolymers reported in literatures such as poly(methyl methacrylate)-*g*-PNIPAM,[28] poly(glycidyl methacrylate)-*g*-PNIPAM,[30] and PCL-*g*-PNIPAM.[31,32] The thermally-triggered micelle aggregation of PVC-*g*-PNIPAM is reversible. As shown in Figure 6a, when the aggregated copolymer micelles is cooled, the aggregate disassociates and the micelle solution becomes transparent again. However, the LCST attained in the cooling process is ~5 °C lower than that obtained from the heating process, meaning that a lower temperature is required to dissociate the micelle aggregate in cooling.

Interestingly, the thermally-triggered micelle aggregation of PVC-*g*-PNIPAM is very unique and the micelles form an aggregate with the well-defined 3D macroscopic shape in the dilution solution (0.3 wt%) upon heating to above LCST (*e.g.*, 40 °C), as shown in Figure 6a. The shape of aggregate is similar to that of the used vessel and the aggregate is nearly cubic when a rectangle cell is used. The aggregate has a similar density as water and it can suspend in the solution. The solution outside the aggregate is transparent, indicating that almost all of the micelles are attached to the formed aggregate. Based on the concentration (0.3 wt%) and bulk density of graft copolymer, it is estimated that the volume fraction of water in micelle aggregate is about 99.6 vol%, demonstrating the extremely high water content in this macroscopic micelle aggregate.
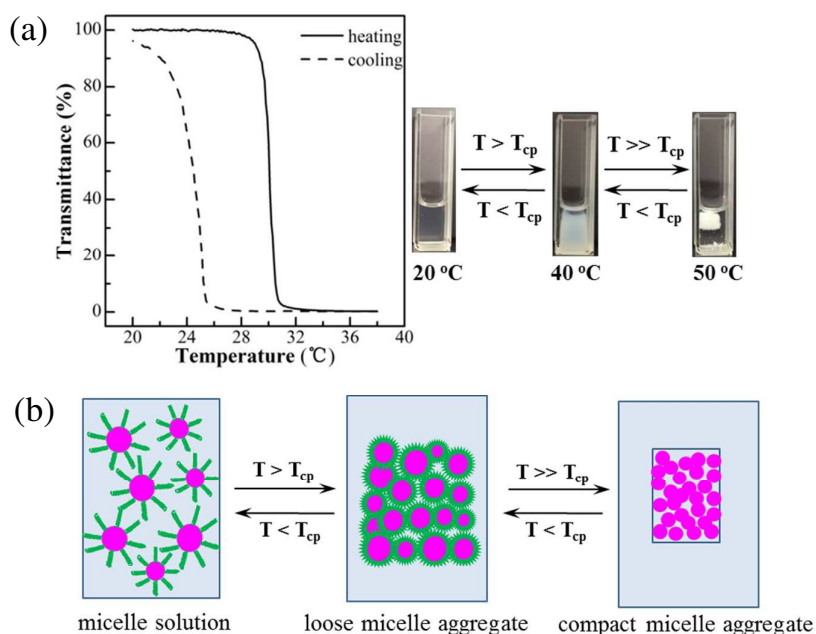
Figure 6. (a) Reversible changes of transmittance and micelle aggregated/dispersed states of PVC$_{149}$-g-PNIPAM$_{46}$ solution (0.3 wt%). (b) Schematic illustration for thermally-induced micelle aggregation of PVC-g-PNIPAM. T_{cp} represents the cloud point or LCST of micelle solution.

As shown in Figure 6a, the micelle aggregate shrinks into a more compact structure as the temperature is increased from 40 to 50 °C. The aggregation process is thermally reversible and the compact aggregate changes to a transparent solution when the temperature is decreased to below LCST. It can be concluded that the thermal-triggered aggregation of PVC-g-PNIPAM is a multistep process. It experiences the micelle solution, loose and compact micelle aggregating states with increasing the temperature, as illustrated in Figure 6b. Below LCST, the PNIPAM grafts are hydrophilic and interact with the surrounded water molecules by hydrogen bonds, which can stabilize the micelles. As the temperature is increased to above LCST, the grafted PNIPAM chains collapse into the globular conformation and the water is expelled out, leading to the increased attractions between micelles. The micelle aggregate is formed and grown in size due to the coagulation driven by the

hydrophobic and van der Waals interactions between micelles. As the temperature is further increased, the water is further expelled out from the micelle aggregate, leading to the formation of more compact aggregate. As the temperature is decreased to below LCST, the grafted PNIPAM chains change from hydrophobic to hydrophilic and the water can gradually permeate into the micelle aggregate, resulting in the re-dispersion of micelles.

It is notable that the multistep aggregation of PVC-*g*-PNIPAM micelles in dilution solution is different from those of PNIPAM homopolymers, block and graft copolymers of PNIPAM (*e.g.*, PCL-*g*-PNIPAM, PNIPAM-*b*-DNA) investigated in our previous studies,[25,26,31,32] which merely turn into the turbid solution but cannot form the aggregate with such well-defined macroscopic shapes in a dilute aqueous solution (< 1.0 wt%) at a temperature above LCST. Exact mechanism for the unique aggregation behavior of PVC-*g*-PNIPAM micelles is still unknown. Plausible reasons for this may be due to the strong hydrophobicity and high density of PVC core, large attractions between micelles, and similar density of micelle aggregates with water.

Effects of concentration, graft length and density on the aggregation behavior of PVC-*g*-PNIPAM micelles were further studied. As shown in Figure 7a, PVC_{149}-*g*-$PNIPAM_{46}$ micelle solution cannot form the macroscopic aggregate but just becomes turbid at a low concentration of 0.075 wt%. At a higher concentration of 0.1 wt%, a small aggregate is formed in the vessel, but the solution outside the aggregate is not transparent enough, indicating the lower extent of aggregation. As the concentration is further increased to 0.2 wt%, a large aggregate with well-defined shape and flat surface is generated. This indicates that there is a critical concentration for macroscopic micelle aggregation, which is around 0.1 wt% for the PVC-*g*-PNIPAM copolymers studied in this work.
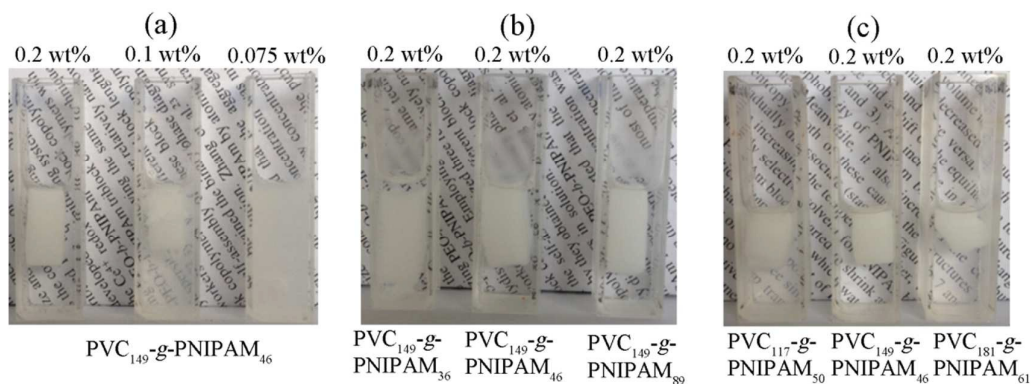
Figure 7. Representative images of macroscopic micelle aggregates form in PVC-*g*-PNIPAM solution with different (a) concentrations, (b) graft lengths and (c) densities after equilibrating at 50 °C for 3 min.

As shown in Figure 7b, at the same graft density or PVC backbone, PVC-*g*-PNIPAM micelles tend to form more compact and well-defined macroscopic aggregates with the increase of graft length or m_{PNIPAM}. This may be due to the fact that the longer graft chains are preferential to bridge the micelles into a large aggregate. In addition, the existence of more PNIPAM chains would also enhance the thermoresponsivity and aggregation ability of micelles. As shown in Figure 7c, when the graft lengths of PNIPAM are similar, a more compact micelle aggregate is formed as the graft density of PVC-*g*-PNIPAM decreases. This could be ascribed to the increased ratio of hydrophobic/hydrophilic segments. The average length of PVC chains between the grafting sites is increased as the graft density decreases, which would lead to the increased hydrophobic interactions and aggregation ability between micelles.

Interestingly, the shape of PVC-*g*-PNIPAM micelle aggregate can be tuned by varying the shape of vessel. As shown in Figure 8a, a cylindrical aggregate is formed when a cylindrical vessel is used. This suggests that the macroscopic aggregation of micelles in the dilute solution is isotropic. To analyze the microstructure, the solution

outside the aggregate was filtered off and the micelle aggregate are freeze-dried to remove the water inside. A free-standing and superporous PVC-*g*-PNIPAM material with a well-defined 3D shape is attained (Figure 8b), which has a density as low as 0.01 g/cm^3. The porosity of free-dried aggregate is estimated by $(1-\rho_0/\rho) \times 100\%$, in which ρ_0 and ρ are the densities of free-dried aggregate and copolymer, respectively. ρ is calculated based on the densities of PNIPAM (1.1 g/cm^3) and PVC (1.4 g/cm^3) homopolymers and their weight fractions. It is calculated that the porosity of free-dried aggregate is larger than 99%. Such low density and high porosity is the typical characteristics of aerogel. As observed by SEM (Figure 8c), the dried aggregate is consisted of the entangled and interconnected copolymer fibrils with a mean diameter less than 500 nm.

| (a) | (b) | (c) |
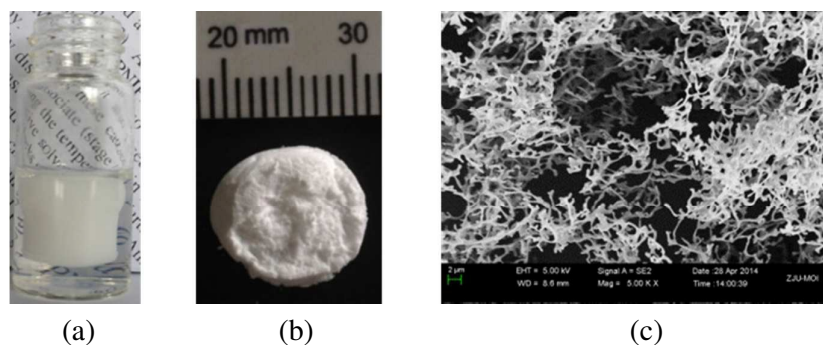
Figure 8. (a) Cylindrical aggregate formed in micelle solution (0.3 wt%, 40 °C), (b) freeze-dried aggregate, and (c) SEM images of freeze-dried aggregate for PVC$_{149}$-*g*-PNIPAM$_{46}$.

Conclusions

PVC-*g*-PNIPAM graft copolymers with different graft lengths and densities were synthesized with a combination of free radical polymerization and SET-LRP. The grafting copolymerization of NIPAM on P(VC-*co*-ABiB) backbone is proceeded in a "living" manner. Chemical structure, micellation, and thermally-induced multistep aggregation of PVC-*g*-PNIPAM copolymers were investigated.

PVC-*g*-PNIPAM copolymers form the micelles consisting of PVC core and PNIPAM corona in water at room temperature. Micelle size and LCST of PVC-*g*-PNIPAMs enhance with increasing the graft density and length of PNIPAM. PVC-*g*-PNIPAM micelles are thermoresponsive and aggregate at a temperature above LCST. As the temperature is increased to above LCST, PVC-*g*-PNIPAM micelles show the unique multistep aggregation behavior and they can form a macroscopic aggregate with well-defined and tunable 3D shape even at an extremely low concentration (~0.1 wt%). The aggregate shrinks to a more compact state upon further heating. After freeze-drying the micelle aggregate, a superporous and free-standing PVC-*g*-PNIPAM material with a low density of ~ 0.01 g/cm^3 and a large porosity of > 99% is obtained. This study has found a new phenomenon for the macroscopic and controllable micelle aggregation of thermoresponsive amphiphilic copolymers in the dilute solution, which may be essential for further understanding and controlling the hierarchical self-assembly and multistep phase transition of amphiphilic copolymers in solution.

References

1   G. Reiss, *Prog. Polym. Sci.*, 2003, **28**, 1107−1170.

2   A. Blanazs, S. P. Armes, and A. J. Ryan, *Macromol. Rapid. Commun.*, 2009, **30**, 267−277.

3   S. H. Yeon, S. H. Ahn, J. H. Kim, K. B. Lee, Y. J. Jeong, and S. U. Hong, *Polym. Adv. Technol.*, 2012, **23**, 516−521.

4   Z. G. Xu, S. Y. Liu, Y. J. Kang, M. F. Wang. *ACS Biomater. Sci. Eng.*, 2015, **1**, 585−592.

5   A. S. Hoffman and P. S. Stayton, *Prog. Polym. Sci.*, 2007, **32**, 922−932.

6   H. Wei, S. X. Cheng, X. L. Zhang, and R. X. Zhuo, *Prog. Polym. Sci.*, 2012, **37**, 237−280.

7   S. Q. Liu, Y. Y. Yang, X. M. Liu, and Y. W. Tong, *Biomacromolecules*, 2003, **4**, 1784–1793.

8   Y. Z. You, C. Y. Hong, W. P. Wang, W. Q. Lu, and C. Y. Pan, *Macromolecules*, 2004, **37**, 9761–9767.

9   M. Hales, C. Barner-Kowollik, T. P. Davis, and M. H. Stenzel, *Langmuir*, 2004, **20**, 10809–10817.

10   C. Choi, S. Y. Chae, and J. W. Nah, *Polymer*, 2006, **47**, 4571–4580.

11   C. Choi, M. K. Jang, and J. W. Nah, *Macromol. Res.*, 2007, **15**, 623–632.

12   G. Wilaiporn, Z. Hui, K. Suda, T. Patrick, and H. Voravee, *J. Polym. Sci., Part A: Polym. Chem.*, 2015, **53**, 1103–1113.

13   X.-L. Sun, P.-C. Tsai, R. Bhat, E. M. Bonder, B. Michniak-Kohn, and A. Pietrangelo. *J. Mater. Chem. B*, 2015, **3**, 814–823.

14   X. J. Loh, Y. L. Wu, W. T. J. Seow, M. N. I. Norimzan, Z. X. Zhang, F. J. Xu, E. T. Kang, K. G. Neoh, and J. Li, *Polymer*, 2008, **49**, 5084–5094.

15   C. Chang, H. Wei, C. Y. Quan, Y. Y. Li, J. Liu, Z. C. Wang, S. X. Cheng, X. Z. Zhang, and R. X. Zhuo, *J. Polym. Sci. Part A: Polym. Chem.*, 2008, **46**, 3048–3057.

16   Quan, C. Y.; Wu, D. Q.; Chang, C.; Zhang, G. B.; Cheng, S. X.; Zhang, X. Z.; and Zhuo, R. X. *J. Phys. Chem. C*, 2009, **113**, 11262–11267.

17   P. J. Sun, Y. Zhang, L. Q. Shi, and Z. H. Gan, *Macromol. Biosci.*, 2010, **10**, 621–631.

18   J. F. Zhou, L. Wang, Q. Yang, Q. Q. Liu, H. J. Yu, and Z. R. Zhao, *J. Phys. Chem.*, 2007, **111**, 5573–5580.

19   X. J. Loh, Z. Zhang, Y. Wu, T. S. Lee, and J. Li, *Macromolecules*, 2011, **42**,

194−202.

20 J. Adelsberger, A. Kulkarni, A. Jain, W. Wang, A. M. Bivigou-Koumba, P. Busch, V. Pipich, O. Holderer, T. Hellweg, A. Laschewsky, P. Müller-Buschbaum, and C. M. Papadakis, *Macromolecules*, 2010, **43**, 2490−2501.

21 J. Adelsberger, I. Grillo, A. Kulkarni, M. Sharp, A. M. Bivigou-Koumba, A. Laschewsky,   P. Müller-Buschbaum, and C. M. Papadakis, *Soft Matter*, 2013, **9**, 1685−1699.

22 W. Q. Chen, H. Wei, S. L. Li, J. Feng, J. Nie, X. Z. Zhang, and R. X. Zhuo, *Polymer*, 2008, **49**, 3965−3972.

23 H. Wei, W. Q. Chen, C. Chang, C. Cheng, S. X. Cheng, X. Z. Zhang, and R. X. Zhuo, *J. Phys. Chem. C*, 2008, **112**, 2888−2894.

24 Z. Yang, J. D. Xie, W. Zhou, and W. F. Shi, *J. Biomed. Mater. Res. A*, 2009, **89A**, 988−1000.

25 P. J. Pan, M. Fujita, W.-Y. Ooi, K. Sudesh, T. Takarada, A. Goto, and M. Maeda, *Polymer*, 2011, **52**, 895−900.

26 P. J. Pan, M. Fujita, W.-Y. Ooi, K. Sudesh, T. Takarada, A. Goto, and M. Maeda, *Langmuir*, 2012, **28**, 14347−14356.

27 S. M. Wang, Z. P. Cheng, J. Zhu, Z. B. Zhang, and X. L. Zhu, *J. Polym. Sci., Part A: Polym. Chem.*, 2007, **45**, 5318−5328.

28 D. X. Wu, X. H. Song, T. Tang, and H. Y. Zhao, *J. Polym. Sci., Part A: Polym. Chem.*, 2010, **48**, 443-453

29 Y. Zhao, H. Y. Gao, G. D. Liang, F. M. Zhu, and Q. Wu, *Polym. Chem.*, 2014, **5**, 962−970.

30 B. Y. Jiang, L. Zhang, J. Yan, Q .Q. Huang, B. Liao, and H. Pang, *J. Polym. Sci., Part A: Polym. Chem.*, 2014, **52**, 2442−2453.

31 M. M. Li, P. J. Pan, G. R. Shan, and Y. Z. Bao, *Polym. Int.*, 2015, **64**, 389–396.

32 M. M. Li, G. R. Shan, Y. Z. Bao, and P. J. Pan, *J. Appl. Polym. Sci.*, 2014, **131**, 41115–41123.

33 K. Endo, *Prog. Polym. Sci.*, 2002, **27**, 2021–2054.

34 W. F. Lee and Y. M. Tu, *J. Appl. Polym. Sci.*, 1999, **74**, 1234–1241.

35 W. F. Lee and Y. M. Tu, *J. Appl. Polym. Sci.*, 2000, **76**, 170–178.

36 H. Yoshioka, M. Mikami, Y. Mori, and E. Tsuchida, *Polym. Adv. Technol.*, 1993, **4**, 519–521.

37 E. Arenas, E. Bucio, G. Burillo, and G. P. Lopez, *Polym. Bull.*, 2007, **58**, 401–409.

38 V. Percec and F. Asgarzadeh, *J. Polym. Sci., Part A: Polym. Chem.*, 2001, **39**, 1120–1135.

39 H. J. Paik, S. G. Gaynor, and K. Matyjaszewski, *Macromol. Rapid Commun.*, 1998, **19**, 47–52.

40 J. H. Xia, S. G. Gaynor, and K. Matyjaszewski, *Macromolecules,* 1998, **31**, 5958.

41 B. M. Rosen and V. Percec, *Chem. Rev.*, 2009, **109**, 5069–5119.

42 E. Turan and T. Caykara, *J. Polym. Sci., Part A: Polym. Chem.*, 2010, **48**, 5842–5847.

43 Y. Deng, J. Z. Zhang, Y. Li, J. Hu, D. Yang, and X. Huang, *J. Polym. Sci., Part A: Polym. Chem.*, 2012, **50**, 4451–4458.

44 V. Percec, A. V. Popov, E. Ramirez-Castillo, M. Monteiro, B. Barboiu, O. Weichold, A. D. Asandei, and C. M. Mitchell, *J. Am. Chem. Soc.*, 2002, **124**, 4940–4941.

45 T. Hatano, B. Rosen, and V. Percec, *J. Polym. Sci., Part A: Polym. Chem.*, 2010, **48**, 164–172.

46   N. Chan, M. F. Cunningham, and R. A. Hutchinson, *J. Polym. Sci., Part A: Polym.*

Chem., 2013, **51**, 3081–3096.

Graphic abstract

PVC-*g*-PNIPAM amphiphilic copolymers with controlled graft lengths and densities are synthesized, which form the unique macroscopic aggregates with the well-defined 3D shapes in dilute aqueous solution above LCST.